Fuel 94 (2012) 448–456

Contents lists available at SciVerse ScienceDirect

Fuel

journal homepage: www.elsevier.com/locate/fuel

An experimental and kinetic study of syngas/air combustion at elevated temperatures and the effect of water addition

Deepti Singh, Takayuki Nishiie, Saad Tanvir, Li Qiao *

School of Aeronautics & Astronautics, Purdue University, West Lafayette, IN 47907, United States

ARTICLE INFO

Article history:
Received 16 May 2011
Received in revised form 22 November 2011
Accepted 30 November 2011
Available online 20 December 2011

Keywords:
Syngas combustion
Elevated temperatures
Water addition
Laminar flame speed

ABSTRACT

Laminar flame speeds of premixed syngas/air mixtures were measured at various fuel equivalence ratios (0.6–3.0), H_2 content of the fuel, and preheat temperatures (298–500 K) using a spherically expanding flame configuration. The measured laminar flame speeds were compared with simulations using with three existing chemical kinetic models – GRI Mech 3.0, H_2/CO Davis Mechanism and San Diego mechanism. Reasonable agreement between computations and measurements was achieved at room temperature that validated the new experimental configuration. However, at higher preheat temperatures discrepancies between computed and measured values were large, especially for fuel rich mixtures. Addition of H_2O to two fuels (H_2/CO = 5/95 and 50/50) up to 40% in the fuel–air mixture was studied to understand the effect of moisture in coal derived syngas. For the H_2/CO = 5/95 fuel, flame speed was observed to increase with up to 20% H_2O addition and then to decrease with any further water addition. However, the higher H_2 content fuel (H_2/CO = 50/50) only showed a decrease in flame speed with an increasing water concentration in the fuel–air mixture. The different trends have been explained as a result of the competing chemical and physical (dilution and thermal) effects of H_2O addition on the syngas flames using sensitivity analyses and by analyzing reaction rates and radical concentrations.

1. Introduction

Synthetic gas (syngas) is a mixture of carbon monoxide and hydrogen in various compositions and can be derived from a number of sources such as coal, biomass gasification or from natural gas during steam reforming [1]. Syngas is a potential clean fuel and is already being used in high efficiency gas turbines in the Integrated Gasification Combined Cycle (IGCC) for power generation. The composition of syngas is dependent mainly on the fuel source from which it is derived and it can contain minor constituents such as CO_2, H_2O, NH_3 and H_2S. Variation in its composition can affect the performance of the system. Therefore, it was considered essential to study the burning properties of syngas over a wide range of compositions and with the presence of minor constituents. The accuracy of kinetic models is critical for the design of clean and efficient gas turbine combustors. Thus, comprehensive assessment of the validity of existing chemical kinetic mechanisms under conditions representative of the operating conditions of advanced gas turbines is required.

Numerous experimental and modeling studies have been reported for syngas. Experimental studies include determination of species profiles [2,3], ignition delay times [4–7] and laminar flame speed measurements [8–17]. Several mechanisms have been developed that can be used to represent the chemical kinetics of CO–H_2 and air mixtures, among which are the GRI Mech 3.0 by Smith et al. [18], the H_2/CO Mech by Davis et al. [19], the San Diego mechanism by Petrova and Williams [20], a reduced reaction mechanism for methane and syngas combustion in gas turbines by Slavinskaya et al. [21], and another H_2/CO kinetic mechanism by Frassoldati et al. [22]. Recently two other mechanisms have been developed by Li et al. [23] and Sun et al. [8] with the latest reaction rate constants.

Laminar burning speed is an important parameter that is commonly used for validation of chemical kinetics. Laminar burning speeds of syngas have already been investigated extensively at normal temperature and pressure, using spherical bombs [8,10,11,13,17], counter-flow twin flame configurations [12,24] and Bunsen burners [15,25]. Considerable accuracy in the prediction of the laminar burning speeds has been achieved for normal temperature and pressure conditions. However, anomalies have been reported at higher temperatures and pressures that are closer to the conditions that exist in gas turbines or burners. Natarajan et al.'s [15] studies of CO–H_2 combustion for fuel lean conditions showed that at high temperatures the measured laminar flame speeds have large discrepancies with numerical simulations using GRI Mech 3.0 and H_2/CO Davis Mechanism. Furthermore, few studies (except [26–28]) have considered the effects of minor species

* Corresponding author. Tel.: +1 765 494 2040; fax: +1 765 494 0307.
E-mail address: lqiao@purdue.edu (L. Qiao).

0016-2361/$ - see front matter © 2011 Elsevier Ltd. All rights reserved.
doi:10.1016/j.fuel.2011.11.058

such as H_2O, which could alter the ignition and combustion behavior of syngas.

The motivation of the present paper is to extend flame speed measurements of syngas for various H_2–CO compositions (5% H_2–95% H_2), equivalence ratios (0.6–3.0), and high temperatures (298–500 K) using a spherical flame configuration. In addition, the effect of addition of H_2O to the fuel mixture at high temperature was investigated. Difference in trends of laminar flame speeds with increasing water percentage, for fuels containing H_2/CO in different ratios has been discussed.

2. Experimental method

The major components of the facility used for the experiments include a spherical combustion chamber placed inside a high temperature oven, a high voltage spark generator, and a Schlieren optical system for recording the flame propagation inside the chamber. A schematic of the experimental facility is shown in Fig. 1. The spherical combustion chamber is made of stainless steel with an inside diameter of 36 cm. The chamber is fitted with two diametrically opposed electrodes made of tungsten wire to provide a spark at the center of the chamber. The gap between these two electrodes is adjustable and the voltage between the two electrodes is controlled by the high voltage spark generator to provide the minimum ignition energy. Two quartz windows, with high durability against pressure and temperature shocks, are mounted on diametrically opposite ends to provide access for viewing the flame. The combustion chamber is placed in a customized oven that can be preheated to a maximum temperature of 650 K using a precise temperature controller. A Z-type Schlieren imaging system has been set up to visualize flame propagation using a high-speed digital camera with a maximum capture rate up to 6600 frames per second.

At the start of an experiment, the chamber was first vacuumed and then the reactant mixture was prepared by filling the chamber with gases at the appropriate partial pressures depending on the desired mixture composition and test pressure. The prepared mixture was allowed to lay undisturbed for 30 min to allow for any disturbances to settle and to ensure complete mixing of the fuel and air by diffusion. A triggering circuit was used to simultaneously trigger the recording on the camera and the spark igniter. For the experiments with water vapor addition, water was preheated in a chamber to vapor phase before being added to the fuel mixture in the combustion chamber. Several thermocouples were installed inside the heated water chamber and on the pipelines between the water chamber and the combustion chamber to ensure the temperature were above the boiling point of water.

Commercial grade compressed air was used for the experiment with 99.5% purity. H_2 and carbon monoxide were graded at 99.8% and 99.5% purity respectively. A recent study by Chaos and Dryer [31] has attributed the deviations between experimental results from different groups to the presence of iron pentacarbonyl ($Fe(CO)_5$) impurities in carbon monoxide. Therefore, carbon monoxide stored in aluminum containers was used in the experiments to ensure the absence of iron pentacarbonyl, a flame inhibitor, as shown by Rumminger and Linteris [30], that develops over time in carbon monoxide stored in steel containers.

3. Data processing

Similar to previous measurements of flame speeds [32,33] for gaseous fuels using a spherical combustion chamber of the same size, flame radius measurements have been limited to a range of 8 mm < r < 30 mm. The lower limit was chosen to avoid disturbances caused by the transient ignition process and the upper limit was to ensure that the pressure increase inside the chamber was negligible. The lower limit was determined experimentally in a manner similar to that employed in the studies of liquid fuels, which was described in a previous paper [34]. The upper limit of 30 mm was imposed on the radius of flame measurements in accordance with past flame speed measurement in a similar configuration [32,35–38]. This value corresponds to 16.67% of the maximum radius and just 0.46% of the total volume of the chamber, which ensures that the pressure rise over this radius is less than 0.7%. Additionally, Burke et al. [39] has shown that for flame radius less than 40% of the maximum, the flame speed is affected by less than 1% due to pressure increase in the chamber. Chen et al.'s [40] theoretical study of a spherically propagating methane/air flame also showed that for a ratio of flame radius to maximum radius lesser than 0.2, the effect of compression induced flow is almost negligible.

Under these assumptions, the local stretched flame speed and flame stretch is given by the following quasi-steady expressions proposed by Strehlow and Savage [41],

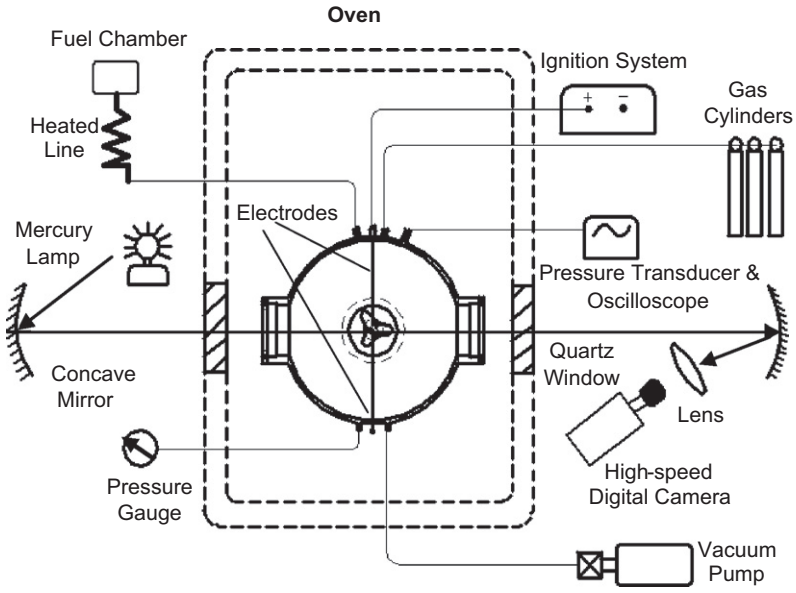

Fig. 1. A schematic of the experimental facility.

$$S_L = \frac{\rho_b}{\rho_u}\frac{dr_f}{dt} \quad (1)$$

$$K = \frac{2}{r_f}\frac{dr_f}{dt} \quad (2)$$

where S_L is the unburned gas speed and K is the flame stretch. The ratio of the burned gas to the unburned gas density was computed using the NASA Chemical Equilibrium Applications code under the assumption of adiabatic constant pressure combustion [42].

For small stretch rates, the stretched flame speed data can be extrapolated linearly to zero stretch to obtain the unstretched laminar flame speed, $S_{L\infty}$. The following equation proposed by Markstein [43] and Clavin [44] provides this linear relationship:

$$S_L = S_{L\infty} - L_u K \quad (3)$$

where L_u is the Markstein length.

This widely-used linear relation (Eq. (3)) is however subject to the limitations of small stretch rate [45]. For moderate stretch rates, the following non-linear relation based on a model developed by Ronney and Sivashinsky [46] for quasi-steady, outwardly propagating spherical flames is more appropriate to obtain the unstretched laminar flame speed ($S_{b\infty}$):

$$\left(\frac{S_b}{S_{b\infty}}\right)^2 \ln\left(\frac{S_b}{S_{b\infty}}\right)^2 = -\frac{2L_b K}{S_{b\infty}} \quad (4)$$

where S_b is the stretched flame speed of the burned gases and L_b is the burned gas Markstein length. The unstretched flame speed relative to unburned gases ($S_{L\infty}$) is related to $S_{b\infty}$ by the ratio of the burned and unburned gas density. For most conditions, the flame speeds obtained by linear and non-linear extrapolation were very similar. The values of flame speeds presented below are obtained using non-linear extrapolation.

4. Computational method

Numerical simulations of steady, laminar, freely propagating 1-D premixed flames were carried out using the PREMIX [47] module of the CHEMKIN 4.1 [48] software. Multi-component diffusion coefficients were used to evaluate the transport properties of the gas mixture. Computational grid and grid tolerance parameters were reduced to 0.1 or lower to ensure accuracy.

Three reaction mechanisms – GRI Mech 3.0 [49], H_2/CO kinetic model proposed by Davis and Law [50] and San Diego mechanism [20] have been used to numerically simulate the laminar burning speeds. The GRI Mech 3.0 contains 53 species and 325 reactions and has been validated by various experimental studies for the accurate prediction of laminar burning speeds, species profiles and ignition delay times of methane–air mixtures and CO–H_2/air mixtures [18]. The second mechanism which is specific to H_2/CO combustion consists of 14 species and 30 reactions [19]. It has been extensively validated for a large number of combustion parameters and is widely cited in literature. It is now the basis of the USC Mech II [51] reaction model for C1–C4 kinetics. The San Diego mechanism consists of 38 species and 235 reactions and has been developed to represent the behavior of various small hydrocarbons containing up to 3 carbon atoms, in conditions that occur in flames, high temperature ignition and detonations. This mechanism has been verified with several gases and fuels to give fairly accurate predictions [52]. Simulations from this mechanism were verified against burning speeds and auto-ignition characteristics of premixed CO/H_2 flames and were shown to have excellent agreement with data available in literature.

5. Results and discussion

The unstretched flame speeds of different H_2–CO mixtures are presented below as a function of equivalence ratio at atmospheric pressure and normal and elevated temperatures. The measured speeds were compared with the numerical simulations using GRI Mech 3.0 [18], H_2/CO Mech [19] and San Diego [20] kinetic mechanisms, as well as experimental data from literature. Furthermore, laminar flame speeds of syngas mixtures with addition of water are reported along with comparisons with computational results and an analysis of the results. In the following discussion the laminar flame speed refers to the unstretched speeds.

5.1. Validation: flame speeds at room temperature

Experiments were performed for various compositions of syngas at 298 K. These results were compared with the experimental data in the literature with the intention of providing a validation for the current experimental setup. Fig. 2 shows the measured and predicted flame speeds for syngas/air mixtures a function of fuel equivalence ratio at 298 K and 1 atm. Also shown are the experimental data of Sun et al. [8], McLean et al. [11] acquired from spherically propagating flames and Natarajan et al. [15] using Bunsen burner flames, where available. For the high hydrogen content (HHC) syngas mixtures (75% H_2–25% CO), no data have been reported previously.

For the 5% H_2–95% CO mixture, all the measurements made using spherically propagating flames (Sun et al. [8] , McLean et al. [11] and the present results) are in good agreement with each other. The values measured by Natarajan et al. [15] are slightly higher than the present measurement and other measurements made with spherical flame configurations over equivalence ratios ranging from 0.6–0.9. Similarly for the 25% H_2–75% CO mixture and the equimolar mixture of H_2–CO (50–50%), the present measurement are in good agreement with those measured by Sun et al. [8], McLean et al. [11] and Natarajan et al. [15]. On comparison of the computational results, it can be seen that the H_2/CO Davis mechanism and the San Diego mechanism can simulate the experimentally determined flame speeds with better accuracy as compared with the GRI Mech-3.0 mechanism. The predictions by the GRI Mech 3.0 [18] are higher than the predictions by the other two mechanisms and the difference is most significant for fuel rich mixtures.

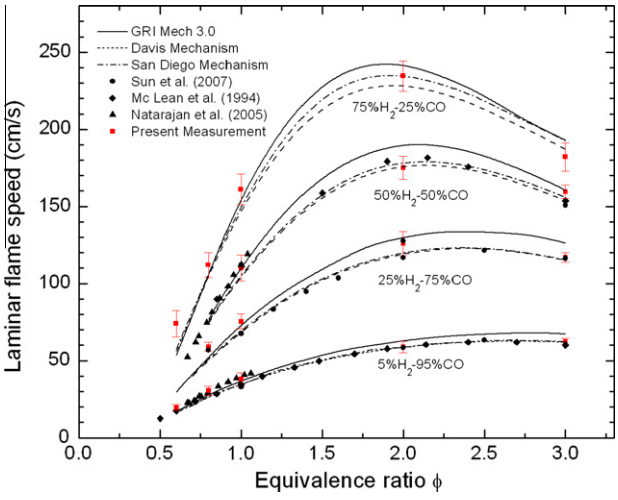

Fig. 2. Laminar flame speeds of various compositions of H_2–CO mixtures for different equivalence ratios at 298 K and 1 atm. Lines represent simulations using different mechanisms and symbols represent experimental data.

With increase in percentage of hydrogen in the fuel mixture, there is an increase in the flame speeds at all equivalence ratios, as expected. The equivalence ratio corresponding to the maximum burning speed shifts towards the fuel lean side with increase in hydrogen content in the fuel. The flame speed peaks at approximately $\phi = 3.0$ at a value close to 65 cm/s for a 5% H_2–95% CO mixture whereas the peak occurs at $\phi = 1.8$ for the 75% H_2–25% CO fuel. The shifting of the peak from rich to lean going from 5% H_2 to 75% H_2 in the fuel mixture is because addition of H_2 to CO results in a kinetic effect through the reaction CO + OH = CO_2 + H. The flame speed has the highest sensitivity to this reaction (as is discussed in Section 5.4). However, this kinetic effect is much stronger for small percentages of H_2 and possibly overshadows the decrease in the flame speed due to reduced adiabatic flame temperatures for the rich mixtures. With higher percentages of H_2, this effect saturates and the peak flame speed is closer to where it occurs for pure H_2 flames.

5.2. Effects of preheat temperature

To examine the effect of preheat temperature on flame speed and chemical kinetics, experiments were conducted at elevated temperatures of 400 K and 500 K for the 50% H_2–50% CO mixture. The results are shown in Fig. 3. With increase in preheat temperature (300–500 K), there is an increase in flame speed as expected. At a preheat temperature of 500 K, the present measurements at fuel-lean conditions are lower than the measurements made by Natarajan et al. [14]. The discrepancy between the measured and computed flame speeds also becomes significant at 500 K, especially at fuel rich conditions. All the mechanisms over predict measured flame speeds.

Discrepancies between measured and predicted flame speeds at higher preheat temperatures have been reported by others for syngas mixtures. Natarajan et al. [15] show that existing kinetics overpredict flame speeds at temperatures above 400 K; and the discrepancy increases with increasing preheat temperature. Note these experiments were conducted primarily for fuel lean conditions. The discrepancies could be due to the inaccurate representation of reaction rates of certain reactions at higher temperatures. Motivated by this, we performed sensitivity analyses of flame speed with respect to reaction rates for the 50% H_2–50% CO mixture at $\phi = 3.0$ at 298 K, 400 K and 500 K, respectively. These results are shown in Fig. 4 and highlight the reactions to which the flame speed is most sensitive. As the preheat temperature increases, the sensitivity coefficient for these reactions increase: $H_2 + O = OH + H$, $H_2 + OH = H_2O + H$ and $H + O_2(+M) = HO_2 + M$. In particular, the last one is a chain recombination reaction involving third bodies. It might be useful to further look at the reaction rates of these reactions at higher temperatures.

5.3. Effect of addition of H_2O

Coal derived syngas from most gasifiers typically has a moisture content of 6–20% [29]. This motivated us to study the effect of water addition on flame speed and chemical kinetics. Stoichiometric fuel mixtures containing H_2–CO in the ratios – 5:95 and 50:50 were used to study the physical and chemical effect of H_2O in syngas. All the experiments were conducted at 400 K. Water was preheated in a heated fuel line to vapor phase before being added to the fuel mixture into the combustion chamber.

Fig. 5 shows the measured and predicted flames speeds for various percentages of water addition to the fuel mixture. An initial increase in flame speed is observed with up to 20% H_2O addition for the fuel mixture containing H_2–CO in a 5:95 ratio. This result is similar to observations made by Das et al. [53] at 323 K. The flame speed from the present measurements at the peak was 28% higher than the flame speed for a dry H_2–CO mixture. Beyond that any addition of water results in a decrease in the flame speed. However, such a trend is not observed for the equimolar mixture of H_2–CO. The flame speed decreases monotonically with H_2O addition in the fuel mixture. The H_2/CO Davis and San Diego mechanisms have better predictions over most of the range of fuel-water mixtures considered for the H_2:CO-5:95 and 50:50 ratio.

The behavior for low H_2 content fuels with H_2O addition was further analyzed to understand the cause of this initial increase in flame speed observed. Fig. 6 shows the calculated adiabatic flame temperature as a function of H_2O percentage in the fuel mixture, for both 5:95 and 50:50 H_2/CO compositions. For both mixtures, the adiabatic flame temperature decreases with increase in H_2O addition, due to the large heat capacity of H_2O, reflecting the physical dilution effect. The decreasing flame temperature should result in a corresponding decrease in flame speed. Therefore, the initial increase in flame speed for low H_2 content fuels with H_2O addition could be due to the dominance of a chemical effect

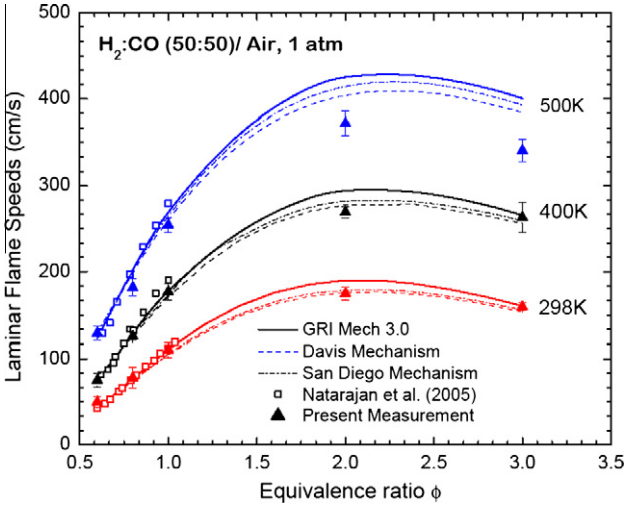

Fig. 3. Comparison of laminar flame speeds for 50% H_2–50% CO at different preheat temperatures at 1 atm. Lines represent simulations using different mechanisms and symbols represent experimental data.

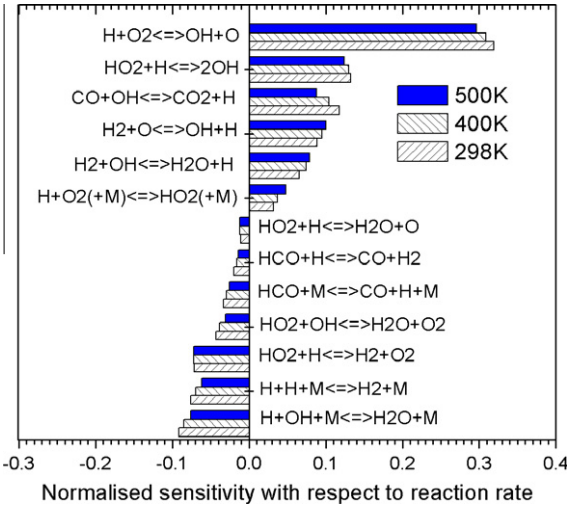

Fig. 4. Normalized sensitivity coefficient of flame speed with respect to the reaction rate for H_2/CO (50:50)/airflames at $\phi = 3.0$ with varying preheat temperature. The sensitivity coefficients were calculated using the San Diego mechanism.

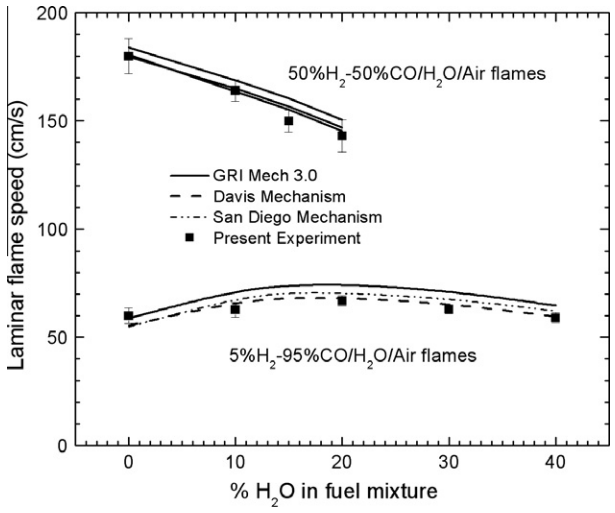

Fig. 5. Laminar flame speeds for H_2/CO(5:95)/H_2O/air flames and H_2/CO (50:50)/H_2O/air at 1 atm and 400 K. Solid lines, dashed and dashed dotted lines represent simulations using GRI Mech 3.0, H_2/CO Davis and San Diego models respectively, and symbols represent experimental data.

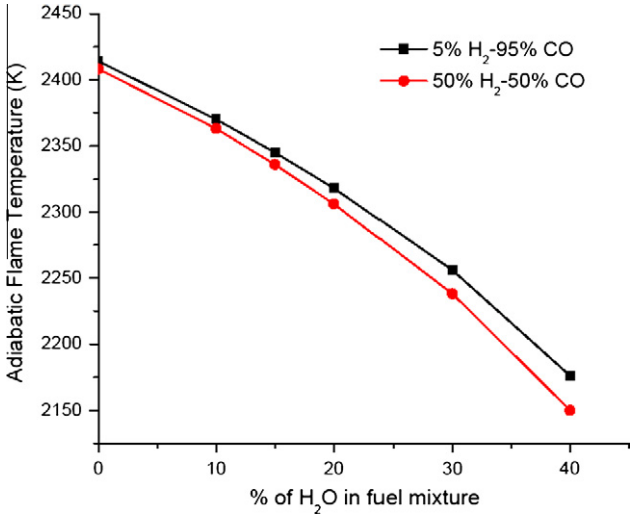

Fig. 6. Calculated adiabatic flame temperature as a function of H_2O percentage in various compositions of H_2/CO/air mixtures.

(e.g., chemical reaction involving H_2O to produce H, O and OH radicals) over this decreasing physical effect [53]. This is discussed in the following.

5.4. Chemical effect of water addition

To understand the chemical effect of water addition, we first examined the concentrations of the important radicals including H, O, and OH in the reaction zone. Previous studies have shown a strong correlation between flame speed and the maximum concentration of H and OH radicals in the reaction zone of premixed hydrogen flames [32,54,55]. Figs. 7 and 8 show the profiles of the intermediate species for H_2–CO (5:95)/H_2O/air and H_2–CO(50–50)/H_2O/air flames respectively, at 1 atm and 400 K using the San Diego Mechanism. For the former flame, the maximum concentration of H and OH radicals increase with H_2O addition up to 20% in the fuel mixture, beyond which the H and OH radical concentrations decreases with further H_2O addition. This indicates that a small amount of water addition produces more H and OH radicals in the reaction zone than the dry fuel. However, the maximum concentration of H and OH radicals decrease monotonically for increasing water percentage to the fuel with 50% H_2–50% CO. For both cases, the maximum concentration of O radical decreases as the water percentage increases. The findings here, which are consistent with the above mentioned earlier studies [32,54,55], partially explain why a small amount of water addition increases flame speed. That is, an increase in H or OH concentrations would result in an increase in flame speed.

To further look at the kinetic effect of water addition, we performed sensitivity analysis of flame speed using the San Diego mechanism. The normalized sensitivity coefficients with respective to the reaction rates of the most important reactions are shown in Fig. 9 for the 5% H_2–95% CO/air mixture. The $CO + OH = CO_2 + H$ (R7) reaction has the highest sensitivity and has an increasing effect on the flame speed with H_2O addition up to 30%. It can be seen that the addition of H_2O increases the sensitivity of the chain branching reactions – $H + O_2 = OH + O$ (R1) and $H_2O + O = 2OH$ (R2), both resulting in an increase in OH radical production. There is decreased sensitivity of the reactions $H_2 + O = OH + H$ (R3) and $HO_2 + H = 2OH$ (R4). The sensitivity to the three-body chain termination reactions $H + OH + M = H_2O + M$ (R5), involving the consumption of OH and H radicals, increases with increase in percentage of H_2O. Since reaction R5 has a negative sensitivity, an increase in its sensitivity indicates a decrease in flame speed with increased reaction rate.

To understand the difference in behavior of the higher hydrogen content fuel, a similar analysis was conducted for the 50% H_2–50% CO mixture (Fig. 10). The major difference is the effect of the reaction $H_2 + OH = H_2O + H$ (R8). In the case of the fuel with H_2/CO in the ratio of 5/95, this reaction has a slight negative sensitivity coefficient on flame speed. With increase in percentage of H_2O the reaction is driven in the reverse direction, generating greater number of OH radicals. On the other hand, for the 50/50 ratio of H_2/CO, the reaction has a strong positive influence. This is because of higher concentration of H_2 that could drive the reaction in the forward direction consuming the OH radicals. The sensitivity of R7 is reduced comparatively and is comparable to the sensitivities of R1 and R2. There is a change in sensitivity of the reactions only with an initial increase in H_2O percentage up to 10% after which the sensitivities remain unchanged. Also, the reaction R2 has an extremely low sensitivity for the 50/50 H_2/CO fuel; whereas it was significant for the previous case indicating that this could be responsible for the difference in behavior of the 2 fuels.

To further understand the chemical effect of water addition, reactions rates were studied, particularly those reactions on which the fuel flow rate has maximum sensitivity. Fig. 11 shows reaction rates of H_2/CO (5/95)/H_2O/air mixtures with H_2O content varying from 0–40%. From the reaction rate profiles, it can be seen that reaction R7 has the highest reaction rate followed by reaction R1. Flame speed has the highest sensitivity to the reaction rate of R7 and this rate almost doubles with 20% addition of water. With any further addition of water, the reaction rate starts to show a very slight decrease. This increase in reaction rate is created by the increased OH radical pool as is seen from the species profiles (Fig. 7). OH radical concentrations show an increase for up to 20% H_2O in the fuel mixture and then slightly decrease. Increased H_2O concentration up to 20% also has an increasing effect on the reaction rates of most of the reactions that result in addition of radicals to the OH pool except reaction R8. The reaction R8 has a negative reaction rate and its rate increases significantly with increase in the percentage of water. The net concentration of OH is a resultant from these reactions causing an increase with up to 20% water addition as is seen from Fig. 7.

In summary, from the above analysis of the reaction rates, radical profiles and sensitivities, it can be seen that addition of water

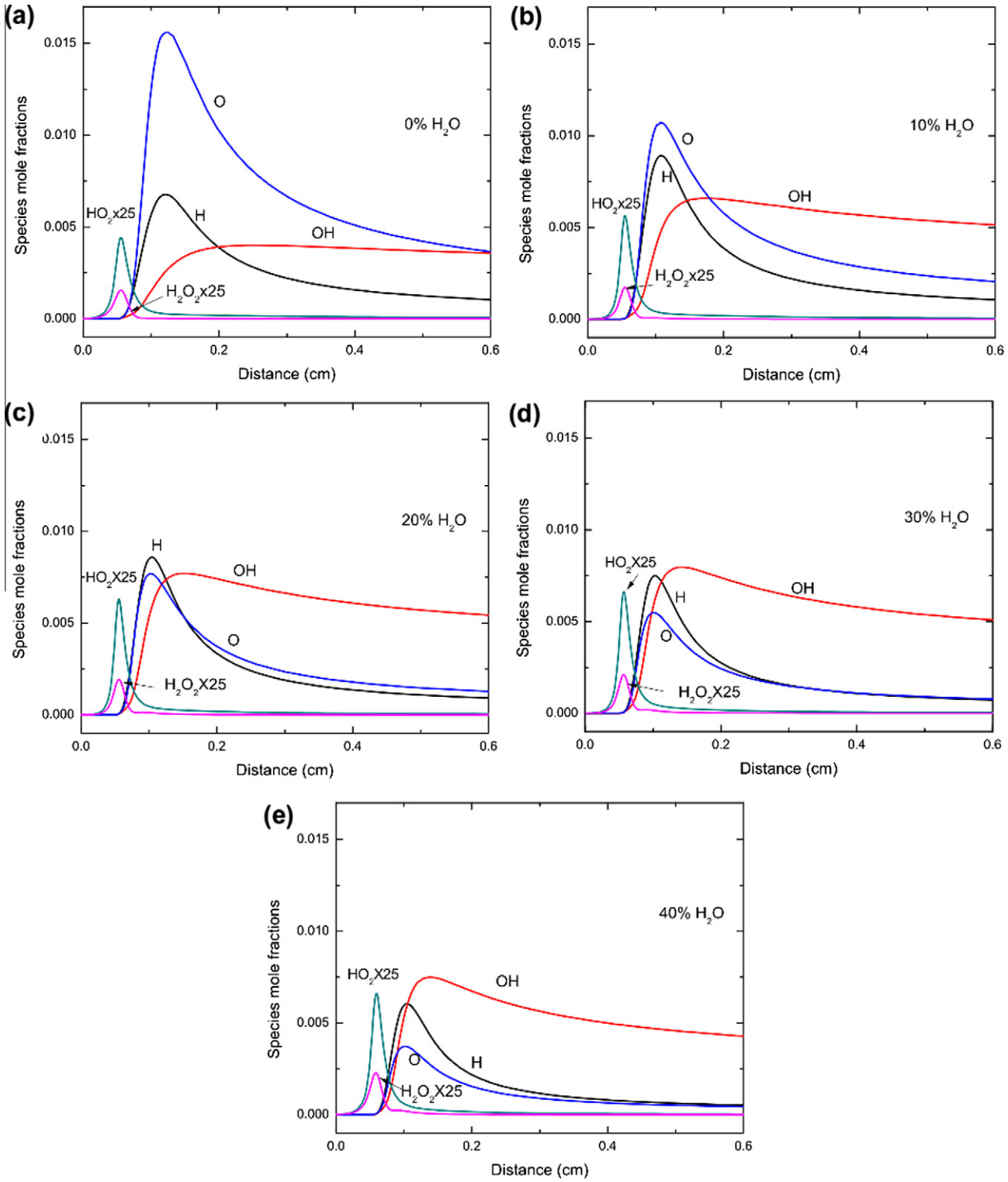

Fig. 7. Profiles of the major radical concentrations for H_2/CO (5:95)/H_2O/air mixtures at 400 K and 1 atm. (a) 0% H_2O; (b) 10% H_2O; (c) 20% H_2O; (d) 30% H_2O; (e) 40% H_2O.

to the fuel mixture (H_2/CO = 5/95) increases the concentration of the OH radicals, which control the main reaction that affects flame speed. The reaction rates depend on reactant temperatures and concentrations of the radicals. With H_2O addition to the fuels, the flame temperatures decrease whereas the OH radical concentrations increase. Therefore, it can be said that for up to 20% H_2O in the fuel mixture, the chemical effect of the increase in OH radicals is stronger than the thermal and dilution effects of reduction in temperature. This results in an increase in the flame speed. Beyond this, the dilution of the fuel and hence, lowering of the flame and burned gas temperature dominates and the resultant effect is a lowering in the flame speed. As opposed to this, the higher H_2 content fuel (H_2/CO = 50/50) does not demonstrate the dominance of chemical effect. The dominant effect on flame speed is the thermal/dilution effect of H_2O presence in the fuel resulting in lowering reaction rates, and therefore, flame speed *s*.

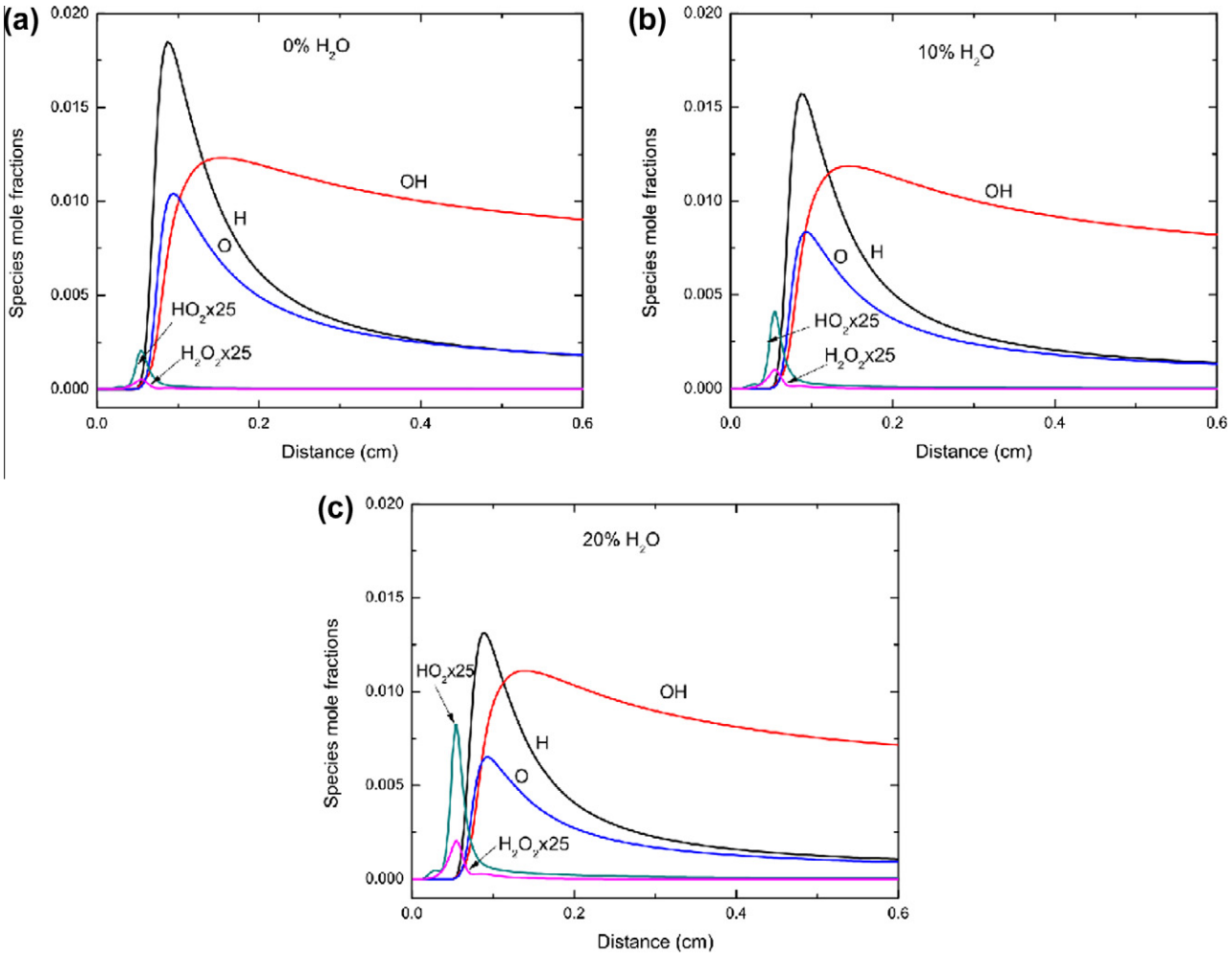

Fig. 8. Profiles of the major radical concentrations for H_2/CO (50:50)/H_2O/air mixtures at 400 K and 1 atm. (a) 0% H_2O; (b) 10% H_2O; (c) 20% H_2O.

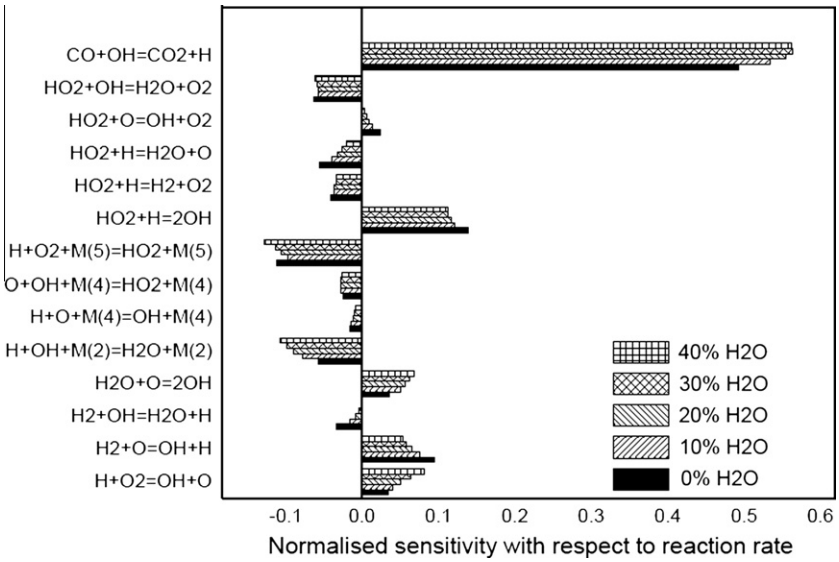

Fig. 9. Normalized sensitivity coefficient of flame speed with respect to the reaction rate for H_2/CO (5:95)/air flames with varying concentration of water (0–40%). The mechanism used is the San Diego mechanism.

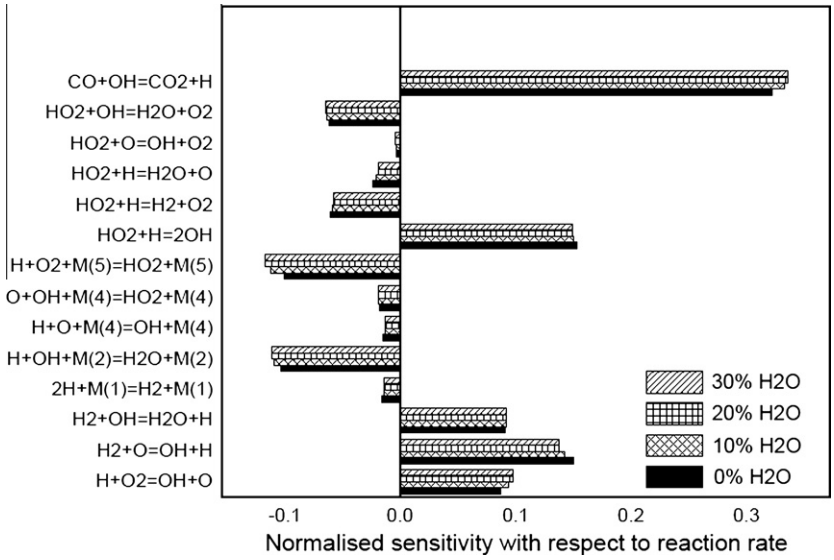

Fig. 10. Normalized sensitivity coefficient of flame speed with respect to the reaction rate for H_2/CO (50:50)/air flames with varying concentration of water (0–40%). The mechanism used is the San Diego mechanism.

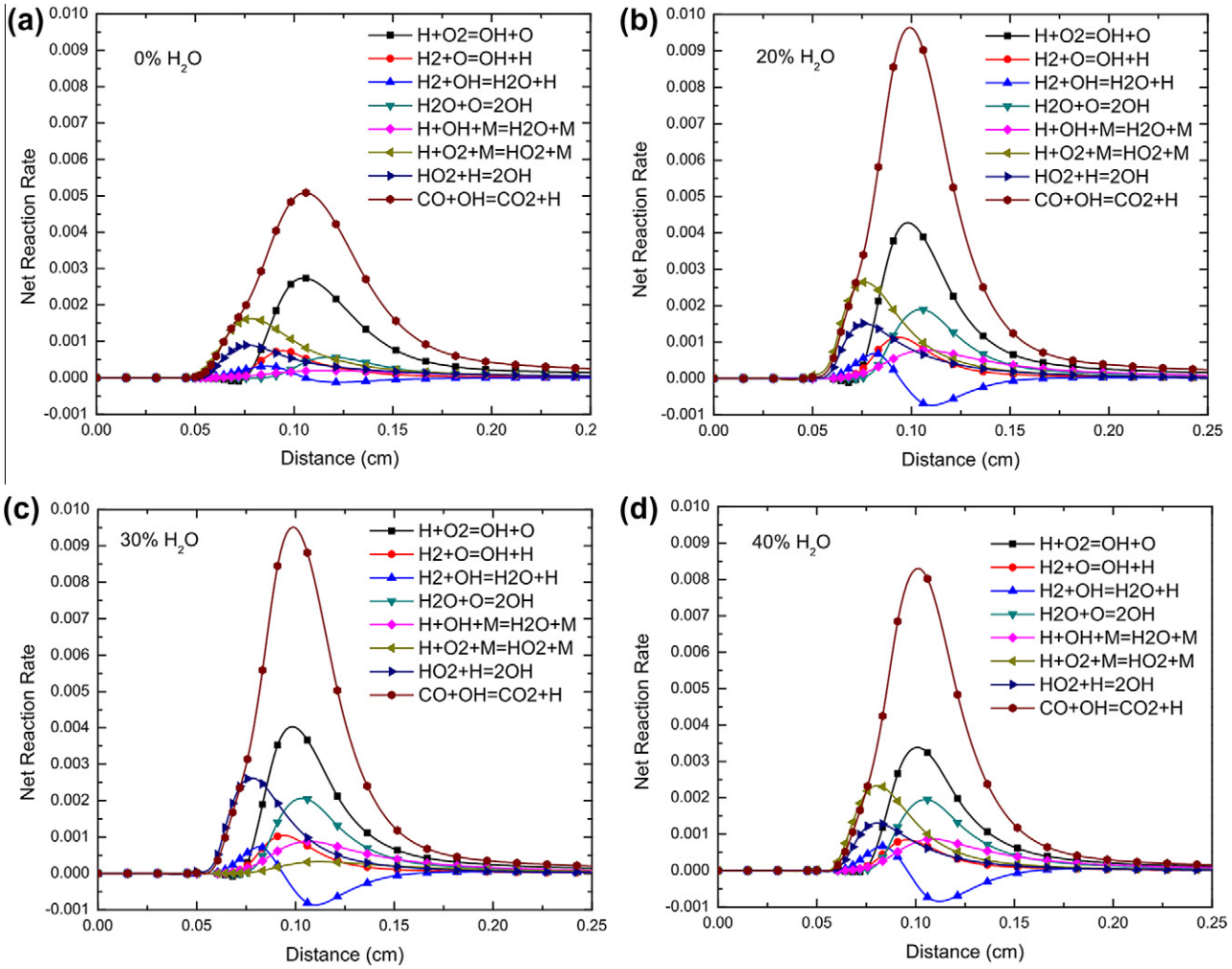

Fig. 11. Reaction rates of the most important reactions for H_2/CO (5:95)/air mixtures with varying percentages of H_2O (0–40%). (a) 0% H_2O; (b) 20% H_2O; (c) 30% H_2O; (d) 40% H_2O.

6. Conclusions

Laminar flame speeds of four compositions of syngas, with H_2 content varying from 5% to 75%, were measured at room and elevated temperatures using spherically expanding flames. The room temperature measurements were in good agreement with the experimental data in the literature, providing a validation of the present experimental apparatus. Large discrepancies between the measured and predicted flame speeds, however, were observed at higher preheat temperatures, especially for fuel rich conditions. The discrepancies could be caused by the inaccurate representation of reaction rates of certain reactions at higher temperatures. Nevertheless, more investigation is needed on the effect of preheat temperature on flame speed and chemical kinetics. Regarding water addition, the low hydrogen content syngas mixture demonstrated an increasing trend with increasing percentage of H_2O in the fuel mixture, up to 20% H_2O addition. Beyond this percentage, the trend reversed and followed the expected behavior due to reduced flame temperature. However, for the high hydrogen content syngas mixture, a straight forward inverse correlation between flame speed and H_2O addition to the fuel mixture was observed. These different trends are attributed to the competition between the chemical effect and the physical effect (thermal and dilution) of water addition.

References

[1] Beychok MR. In: Coal Gasification and the Phenosolvan Process, American Chemical Society 168th National Meeting, Atlantic City, September, 1974; Atlantic City; 1974.
[2] Yetter RA, Dryer FL, Rabitz H. Combust Sci Technol 1991;79(1–3):129–40.
[3] Dagaut P, Lecomte F, Mieritz J, Glarborg P. Int J Chem Kinet 2003;35(11):564–75. doi:10.1002/kin.10154.
[4] Walton SM, He X, Zigler BT, Wooldridge MS. Proc Combust Inst 2007;31:3147–54. doi:10.1016/j.proci.2006.08.059.
[5] Petersen EL, Kalitan DM, Barrett AB, Reehal SC, Mertens JD, Beerer DJ, et al. Combust Flame 2007;149(1–2):244–7. doi:10.1016/j.combustflame.2006.12.007.
[6] Mittal G, Sung CJ, Yetter RA. Int J Chem Kinet 2006;38(8):516–29. doi:10.1002/kin.20180.
[7] Dean AM, Steiner DC, Wang EE. Combust Flame 1978;32(1):73–83.
[8] Sun H, Yang SI, Jomaas G, Law CK. Proc Combust Inst 2007;31(1):439–46.
[9] Hassan MI, Aung KT, Faeth GM. Combust Flame 1998;115(4):539–50.
[10] Hassan MI, Aung KT, Faeth GM. J Propulsion Power 1997;13(2):239–45.
[11] McLean IC, Smith DB, Taylor SC. Int Symp Combust 1994;25(1):749–57.
[12] Vagelopoulos CM, Egolfopoulos FN. Int Symp Combust 1994;25(1):1317–23.
[13] Brown MJ, McLean IC, Smith DB, Taylor SC. Twenty-Sixth Int Symp Combust 1996;1 and 2:875–81.
[14] Natarajan J, Kochar Y, Lieuwen T, Seitzman J. Proc Combust Inst 2009;32(1):1261–8.
[15] Natarajan J, Lieuwen T, Seitzman J. Combust Flame 2007;151:104–19. doi:10.1016/j.combustflame.2007.05.003.
[16] Burke MP, Chaos M, Dryer FL, Ju Y. Combust Flame 2010;157(4):618–31.
[17] Prathap C, Ray A, Ravi MR. Combust Flame 2008;155(1–2):145–60. doi:10.1016/j.combustflame.2008.04.005.
[18] Smith GP, Golden DM, Freklach M, Moriarty NW, Eiteneer B, Goldenberg M, Bowman CT, Hanson RK, Song S, Gardiner Jr WC, V. V. Lissianski, Z. Qin. Available from: http://www.me.berkeley.edu/gri_mech.
[19] Davis SG, Joshi AV, Wang H, Egolfopoulos F. Proc Combust Inst 2005;30(1):1283–92.
[20] Petrova MV, Williams FA. Combust Flame 2006;144(3):526–44. doi:10.1016/j.combustflame.2005.07.016.
[21] Slavinskaya N, Braun-Unkhoff M, Frank P. J Eng Gas Turb Power – Trans ASME 2008;130(2). doi:10.1115/1.2719258.
[22] Frassoldati A, Faravelli T, Ranzi E. Int J Hydrogen Energy 2007;32:3471–85.
[23] Li J, Zhao ZW, Kazakov A, Chaos M, Dryer FL, Scire JJ. Int J Chem Kinet 2007;39(3):109–36. doi:10.1002/kin.20218.
[24] Som S, Ramirez AI, Hagerdorn J, Saveliev A, Aggarwal SK. Fuel 2008;87(3):319–34. doi:10.1016/j.fuel.2007.05.023.
[25] Dong C, Zhou Q, Zhao Q, Zhang Y, Xu T, Hui S. Fuel 2009;88(10):1858–63.
[26] Das AK, Kumar K, Sung CJ. In: Laminar flame speeds of moist syngas mixtures, 6th U.S. National Combustion Meeting, University of Michigan, Ann Arbor, 2009; University of Michigan, Ann Arbor; 2009.
[27] Bunkute B. Burning Velocities of Coal-derived syngas mixtures. Cranfield University; 2008.
[28] Kim TJ, Yetter RA, Dryer FL. Int Symp Combust 1994;25(1):759–66.
[29] Gupta P, Velazquez-Vargas LG, Fan L-S. Energy Fuels 2007;21(5):2900–8. doi:10.1021/ef060512k.
[30] Rumminger MD, Linteris GT. Combust Flame 2000;120(4):451–64.
[31] Chaos M, Dryer FL. Combust Sci Technol 2008;180(6):1053–96.
[32] Qiao L, Kim CH, Faeth GM. Combust Flame 2005;143(1–2):79–96. doi:10.1016/j.combustflame.2005.05.004.
[33] Qiao L, Gu Y, Dam WJA, Oran ES, Faeth GM. Combust Flame 2007;151:196–208. doi:10.1016/j.combustflame.2007.06.013.
[34] Singh D, Nishiie T, Qiao L. Experimental and kinetic modeling study of the combustion of n-decane, Jet-A, and S-8 in laminar premixed flames. Combust Sci Technol 2011;183(10):1002–26.
[35] Kwon S, Tseng LK, Faeth GM. Combust Flame 1992;90(3–4):230–46.
[36] Tseng LK, Ismail MA, Faeth GM. Combust Flame 1993;95(4):410–26.
[37] Aung KT, Hassan MI, Faeth GM. Combust Flame 1997;109(1-2):1–24.
[38] Hassan MI, Aung KT, Kwon OC, Faeth GM. J Propulsion Power 1998;14(4):479–88.
[39] Burke MP, Chen Z, Ju YG, Dryer FL. Combust Flame 2009;156(4):771–9. doi:10.1016/j.combustflame.2009.01.013.
[40] Chen Z, Burke MP, Ju Y. Combust Theory Modell 2009;13(2):343–64. doi:10.1080/13647830802632192.
[41] Strehlow RA, Savage LD. Combust Flame 1978;31(2):209–11.
[42] Gordon S, McBride BJ. NASA Chemical Equilibrium with Applications (CEA).
[43] Markstein GH. Nonsteady flame propagation. New York: Pergamon Press; 1964.
[44] Clavin P. Progr Energy Combust Sci 1985;11(1):1–59.
[45] Kelley AP, Law CK. Combust Flame 2009;156(9):1844–51. doi:10.1016/j.combustflame.2009.04.004.
[46] Ronney PD, Sivashinsky GI. Siam J Appl Math 1989;49(4):1029–46.
[47] Kee RJ, Grcar JF, Smooke MD, Miller JA. in: Sandia National Laboratories: Livermore; 1985.
[48] Kee RJ, Rupley FM, Miller JA, Coltrin ME, Grcar JF, Meeks E, Moffat HK, Lutz AE, Dixon-Lewis G, Smooke M, Warnatz J, Evans GH, Larson RS, Mitchell RE, Petzold LR, Reynolds WC, Caracotsios M, Stewart WE, Glarborg P, Wang C, McLellan CL, Adigun O, Houf WG, Chou CP, Miller CF, Ho P, Young PD, Young DJ, Hodgson DW, Petrova MV, Puduppakkam KV. In: Reaction Design: San Diego, CA; 2007.
[49] Agosta A, Cernansky NP, Miller DL, Faravelli T, Ranzi E. Exp Therm Fluid Sci 2004;28(7):701–8. doi:10.1016/j.expthermflusci.2003.12.00.
[50] Davis SG, Law CK. Combust Sci Technol 1998;140(1–6):427–49.
[51] Wang H, You X, Joshi AV, Davis SG, Laskin A, Egolfopoulos F, Law CK. In: May editor.; 2007.
[52] Saxena P, Williams FA. Combust Flame 2006;145(1–2):316–23. doi:10.1016/j.combustflame.2005.10.004.
[53] Das AK, Kumar K, Sung C-J. Combust Flame 2011;158(2):345–53.
[54] Padley PJ, Sugden TM. Int Symp Combust 1958;7(1):235–42.
[55] Lewis B, Elbe Gv. Combustion flames and explosion of gases. New York: Academic Press; 1987.